Title

Spectral imaging in preclinical research and clinical pathology

Journal

Analytical Cellular Pathology, 35(5,6)

ISSN

2210-7177

Authors

Levenson, Richard

Beechem, Joseph

McNamara, George

Publication Date

2012

DOI

10.3233/acp-2012-0062

Analytical Cellular Pathology 35 (2012) 339–361
DOI 10.3233/ACP-2012-0062
IOS Press

Review Article: Modern Trends in Imaging X

Spectral imaging in preclinical research and clinical pathology

Richard Levenson[a,*], Joseph Beechem[b] and George McNamara[c]
[a]*Pathology and Laboratory Medicine, University of California Davis, Sacramento, CA, USA*
[b]*Genetic Systems, Life Technologies, Foster City, CA, USA*
[c]*Analytical Imaging Core, University of Miami School of Medicine, Miami, FL, USA*

Abstract. Spectral imaging methods are attracting increased interest from researchers and practitioners in basic science, preclinical and clinical arenas. A combination of better labeling reagents and better optics creates opportunities to detect and measure multiple parameters at the molecular and cellular level. These tools can provide valuable insights into the basic mechanisms of life, and yield diagnostic and prognostic information for clinical applications. There are many multispectral technologies available, each with its own advantages and limitations. This chapter will present an overview of the rationale for spectral imaging, and discuss the hardware, software and sample labeling strategies that can optimize its usefulness in clinical settings.

Keywords: Image analysis, immunofluorescence, immunohistochemistry, machine-vision, multispectral imaging, oncology, pathology, personalized medicine, segmentation

1. Opportunities in pre-clinical and clinical tissue analysis

The tasks facing pathologists have multiplied in recent years. Diagnosis (their traditional deliverable) has mainly relied on principles derived from correlative morphology; now, however, pathologists are asked to go beyond assigning labels to lesions, and to provide refined prognosis, therapeutic guidance and even treatment monitoring via a series of biopsies or fine-needle aspirations of unresected primaries or metastases. In the realm of translational research, pathology is called upon to validate other forms of imaging and detection, some of these molecularly based, as well as to guide drug development from early pre-clinical to late, post-approval clinical stages [1]. Many of these new roles depend on detecting the abundance and possibly the activation state of an increasing number of molecules-of-interest present in tissue samples. If such molecules can be correlated with appropriate drug choice and patient outcome, and can navigate through the FDA (or equivalent) approval process, they become so-called "companion diagnostics" and their assay may be mandated as part of a therapeutic regimen especially as they tie in with individualized patient profiling and drug selection [2]. These new tasks may outstrip the capability of conventional pathology reagents and imaging tools, especially, as is increasingly the case, when the amount of available tissue is limiting. Fortunately, relatively new reagents, methods and software approaches have been developed that can help address these challenges. (Disclaimer: due to space- and author-limitations, related approaches using FRET (Förster resonance energy transfer) or FLIM (fluorescence lifetime imaging microscopy) will not be discussed here).

New molecular targets for research, diagnosis or screening (often called "biomarkers") are being identified, seemingly daily, and while some of these are detectable in body fluids (or even in exhaled breath), many of them are most informative when visualized in largely intact cells and tissue. Tissue-based detection of molecular events takes advantage of accumulated experience developed through decades of examining

*Corresponding author: Richard Levenson, Pathology and Laboratory Medicine, University of California Davis, Sacramento, CA, USA. E-mail: Levenson@ucdavis.edu.

samples stained with standard histology dyes [3, 4] — consequently, a molecular phenotype can be interpreted with the help of a rich biological context. Compatible, histology-based imaging methods include immunofluorescence (IF) and immunohistochemistry (IHC) [5]; their development during mid-to-late-20th century ushered in the era of true molecular pathology. Antibody-based methods can go beyond antigen localization to provide information on protein post-translational modifications such as phosphorylation and de-phosphorylation. Such alterations are known to play important roles in signaling pathways [6–14] and function in a complex web of positive- and negative-feedback [8, 9, 11, 12, 14–17]. It is probable that similar relevant molecular assays may eventually become part of the practice of clinical anatomic pathology, but the current lack of consensus on which assays to use confirms the complexity and heterogeneity of cancer progression and underscores a need for new approaches [18–23], perhaps focusing on so-called driver molecules [24]. On the nucleic acid side, conventional *in-situ* hybridization techniques targeting DNA and mRNA have been recently been extended to include non-coding RNAs such as miRNAs and lincRNAs [25–27].

2. Why use microscope-based imaging for molecular phenotyping?

As appreciation of the complexity of disease-relevant molecular interactions has deepened, so has the need for techniques that can look at more than one analyte at a time. Such molecular phenotyping can be image-based, or it can rely on techniques that extract molecules from their native location before assaying them. Imaging tissue, with IHC or IF, for example, can be slow, complex and subject to a host of confounding problems with tissue preparation and molecular detection, and are limited to the number of molecules that can be simultaneously detected. In contrast, other extremely powerful and exciting multiplexed molecular analysis methods, which now include proteomic techniques and targeted or deep whole genome sequencing, can survey hundreds to millions of molecular events in parallel from a single specimen. There is no doubt that such approaches will have unforeseeable and profound impacts on biology and medicine, but because these techniques are largely not informed by spatial context, major insights may be lost and quality assurance is made more difficult. One problem is posed by sample heterogeneity. If the detection systems do not have good dynamic range, molecular phenotypes representing the bulk population can swamp out real but small signals from small cell populations [28, 29]. These minority populations can be of potentially greatest interest, as in the case of cancer stem cells thought to represent a small but critical part of a tumor ecosystem. Secondly, it is not always the case that the signal seen actually came from the cells intended to be the investigation target. For example, some samples of tissue submitted for genomic analysis may have actually little or no tumor present, or the tumor cells may be so diluted by host-derived cells that the measured phenotype becomes difficult to interpret. Some of these problems can be addressed via careful sample preparation, including laser capture microdissection [30, 31].

Microscopic-based imaging, on the other hand, while not achieving the depth of molecular coverage that the ensemble techniques can generate, nevertheless can provide unique and/or complementary information. First of all, the fact that single cells can be visualized means that even rare cell populations can be studied without their signals being swamped by those of the majority. Individual Hodgkin's cells can be detected and studied even when surrounded by a sea of reactive immune cells [32]. A related advantage is that all components of an important and complicated microenvironment can be examined simultaneously, providing insight into biological cross-talk present at the tumor-host interface [33]. Also, the image itself provides validation that the tissues being examined are in fact the intended ones. Perhaps more importantly, image-based techniques can yield molecular information with spatial precision that spans many orders of magnitude, from the subcellular level (even to single-nanometer scale) all the way up to whole organs. Moreover, such spatial precision gains extra value when several molecules (or cell types) can be detected simultaneously and their location with respect to one another evaluated.

To the extent that antibody panels [34, 35] are usually assayed using many serial sections can be multiplexed instead onto a single slide, there could be benefits realized in workflow, cost and case-review effort. Advantages of multiplexing are even greater when only limited sample is available. Not only can more information be obtained from less tissue, but correspondingly more tissue is then available for other

molecular tests. Unfortunately, recent changes in reimbursement policies in the US that discourage the use of multiple stains on single slides may strongly work against this trend, at least in the short run.

3. Bright field vs. fluorescence (or IHC vs. IF)

There is an on-going debate as to the relative merits of bright field vs. fluorescence when it comes to performing molecular detection in tissue. Pathology still relies almost exclusively on the traditional microscope, with light projected through the sample towards the eyepieces or camera (bright field mode). Contrast is generated by absorption and scattering, typically by organic stains such as hematoxylin and eosin, and/or by chromogens (colored labels) deposited at or near molecular targets. Fluorescence, which uses light emission, rather than absorption, is by contrast, the dominant technique in basic research settings, but is rarely found in the clinic—with the exception of some relatively low-volume skin and renal immunopathology applications and fluorescence *in-situ* hybridization (FISH) assays for HER2 amplification. The situation may eventually change because fluorescence-based techniques have the potential for increased sensitivity, improved dynamic range, suitability for high levels of multiplexing even when signals are overlapped, no requirement for enzymatic amplification (and therefore, improved linearity) and potential for single-cocktail labeling approaches [36].

New labeling reagents have increased the possible utility and clinical acceptability of fluorescence techniques. The advent of quantum dots (QDs), semi-conductor-based fluorescent nanoparticles, for example, was expected to boost clinical utilization of fluorescence due to these agents' relative resistance to photobleaching and reasonable stability in stained samples; their simplified optical requirements (single excitation wavelength), and reports of successful tissue-based multiplexing [37–39] led to early enthusiasm. However, quantum-dot-based labels have not yet achieved widespread adoption, in part due to their own properties as well as to other challenges that fluorescence-based methods face in general [38]. One of these is interference from various sources of autofluorescence, especially common with formalin-fixed tissue samples [40–45]. Additional hurdles include the requirement for complex and expensive microscopes, and interference with typical pathology workflow. Equally importantly, fluorescently stained specimens do not resemble familiar bright field samples, and because they frequently do not include a non-nuclear counterstain (essentially, an eosin equivalent), it can be very hard to see beyond the possibly sparse labels to appreciate what the sample actually looks like.

The much more popular bright-field chromogenic (colored) stains that only absorb rather than emit light have their own set of advantages and drawbacks. Most notably, especially when counterstained, the samples appear familiar, and provide good spatial context for the molecular signals. The stains are relatively stable and do not require special storage or viewing stations. It is a major challenge, however, to achieve reproducible staining intensities with typical enzymatically enhanced chromogen deposition (a non-linear process sensitive to reaction conditions), and comparisons on inter-institutional staining and interpretation of IHC samples have often demonstrated low agreement levels [46], although reasons for irreproducibility involve far more than just the chromogen deposition step. On the plus side, the optical measurement of the absorbing molecules can be done in optical-density mode, which should yield instrument-independent values. This property can facilitate robust inter-institutional comparisons (assuming the sample preparation and staining methodologies are well controlled [47]). A major disadvantage of bright field molecular imaging is that, without some form of enhanced spectral discrimination, it can be difficult to impossible to resolve multiple overlapping colors and obtain even qualitative data from multiplexed chromogenically stained samples.

4. Standard microscopy and its discontents

Many pathologists may feel that additional tools beyond just a microscope, their own eyes, and possibly a digital camera, are not actually needed, and they are concerned that novel, potentially expensive and intrusive technology may not be worth its cost in either money or time. But as the number of simultaneous molecular targets examined goes up, the limitations of standard imaging methods become increasingly apparent.

The spectral resolution of the human retina (and RGB cameras) is limited to 3 major and overlapping spectral ranges (red, green, blue). The sensations of colors arise from differential stimulation of these 3

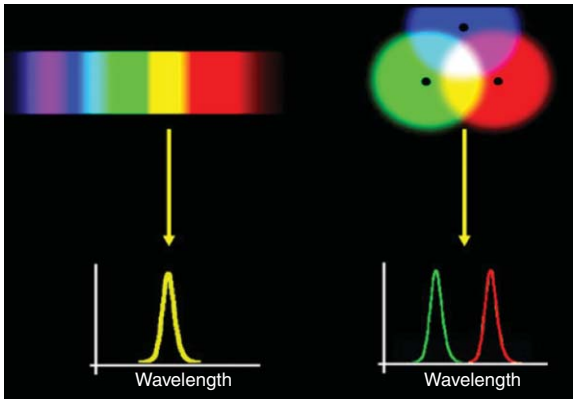

Fig. 1. Color and spectral content are not synonymous.

receptors, and it should not come as a surprise that there might be more than one way to stimulate the receptors to equivalent activation levels. For example, the sensation, "yellow," arises when the red and green receptors receive equal stimulation. This can be accomplished by a near-infinite set of combinations of other wavelengths in the green-red range, a phenomenon known as metamerism [48]. Obviously, this redundancy only deepens when more than two signals spatially overlap, and is true in both fluorescence (additive) and bright field (subtractive) color environments.

Conventional fluorescence imaging based on monochrome cameras and appropriate narrow-band filters would have no problems distinguishing a true yellow emitter from red-plus-green signals; nevertheless, this optical set-up is still challenged by the broad emission spectra (and long red tails) of most organic fluorochromes, leading to overlap or crosstalk between channels. It is difficult to design a set of filters with acceptable light-throughput that can transmit light coming from just one fluorescent species while completely blocking that of another. While good separation can be achieved using multiple filter sets in standard fluorescence microscopes (up to 6 can be installed in typical research system), and even greater flexibility is available if filter wheels on both the excitation and emission paths are used [49], such flexibility involves increased cost and complexity.

Hard-to-resolve mixtures of fluorescent signals in many or most separate channels can be inevitable when autofluorescence is present. Autofluorescence is the often-unwanted spontaneous fluorescence emission of the cells or tissues being imaged not arising from the exogenous dyes used for labeling [44, 45]. Autofluorescence is typically broad, extending a hundred nanometers or more, and can be intense, especially with plants, insects, worms, fish, neurons and formalin-fixed tissues in general. It results in a greenish-yellow haze with conventional red or green filter sets and can decrease contrast or overwhelm weak signals entirely. While a number of approaches to getting rid of autofluorescence chemically have been developed [42–45, 50], they may not be particularly effective or generally applicable. The intensity of autofluorescence drops dramatically when the sample is excited in the red and near-infrared regions, a phenomenon that has motivated the development of fluorochromes emitting in the far-red. However, the availability of NIR dyes does not solve the problem of spectral overlap and autofluorescence in the much more populated visible range.

5. Spectral imaging can help

Spectral imaging (also referred to as multispectral or hyperspectral imaging) is a technique that has been used in research and development in the biosciences since the 1990 s, and is finally gaining traction as the hardware and software have improved, additional application needs are emerging, and convenient multispectral reagents, including quantum dots and appropriately labeled primary antibodies, are becoming available. Some of the hardware and software approaches will be outlined below. Simply put, the technique provides a spectrum (with variable spectral resolution) at every pixel of an image. Analysis is based on well-validated standard spectroscopic algorithms used for decades for detecting, "unmixing" and quantitating components in mixtures; spectral imaging software essentially adapts those approaches to provide pixel-by-pixel quantitative data. What spectral imaging offers over conventional methods is improved *detection*, *validation*, *separation*, and *quantitation* [40, 51, 52].

5.1. Detection

Autofluorescence, if sufficiently bright, can completely mask the presence of desired signals. Somewhat paradoxically, spectral imaging, although less light-efficient overall than typical microscopy techniques, can increase sensitivity due to the increased information content of the captured signals, and can

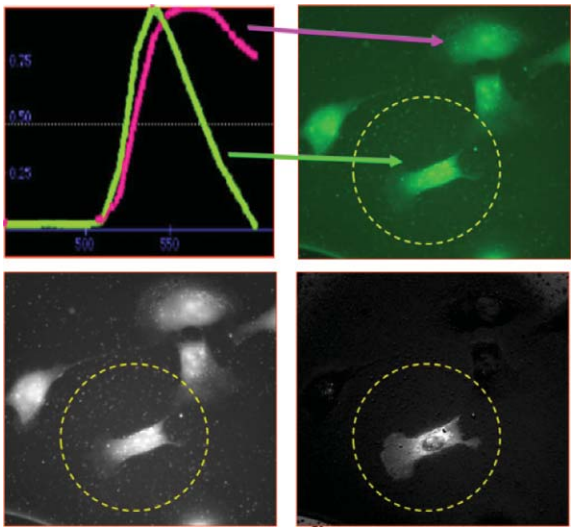

Fig. 2. Removal of autofluorescence reveals an otherwise undetectable YFP+ transfected cell.

detect otherwise invisible, or rather, indistinguishable, targets. An example is given in Fig. 2, which shows a number of cells with autofluorescence, only one of which was expressing yellow fluorescent protein (YFP). Using the spectrum of the autofluorescence and YFP spectrum alone, the image can be separated to reveal the autofluorescence signals (all cells equally bright, predominantly nuclear, low contrast) and the single YFP-positive cell, whose signals are predominantly cytoplasmic. In this case, the YFP signal in the positive cell was present at only about one-tenth the level of the autofluorescence.

5.2. *Validation (or identification)*

By having the spectral characteristics associated with each channel, a user can confirm, for example, that the green signals in their specimen that look so promising are indeed generated by a fluorescent label, such as Alexa Fluor 488 or green fluorescent protein, for example, rather than being simply brightly autofluorescent tissue elements. The latter may often appear greenish (especially through a narrow-band emission filter), but will almost certainly have a detectable optical spectrum easily distinguished from that of the fluorescent label (see spectra in Fig. 2). Shown in Fig. 3, a formalin-fixed, paraffin-embedded section of highly autofluorescent prostate tissue was stained for

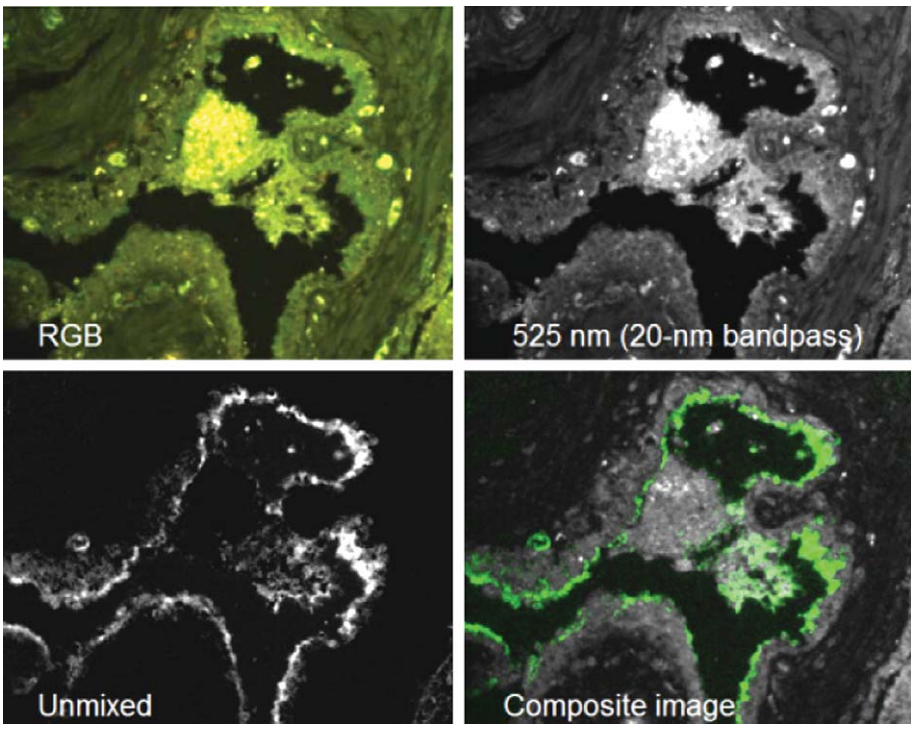

Fig. 3. Removal of autofluorescence reveals dim signals.

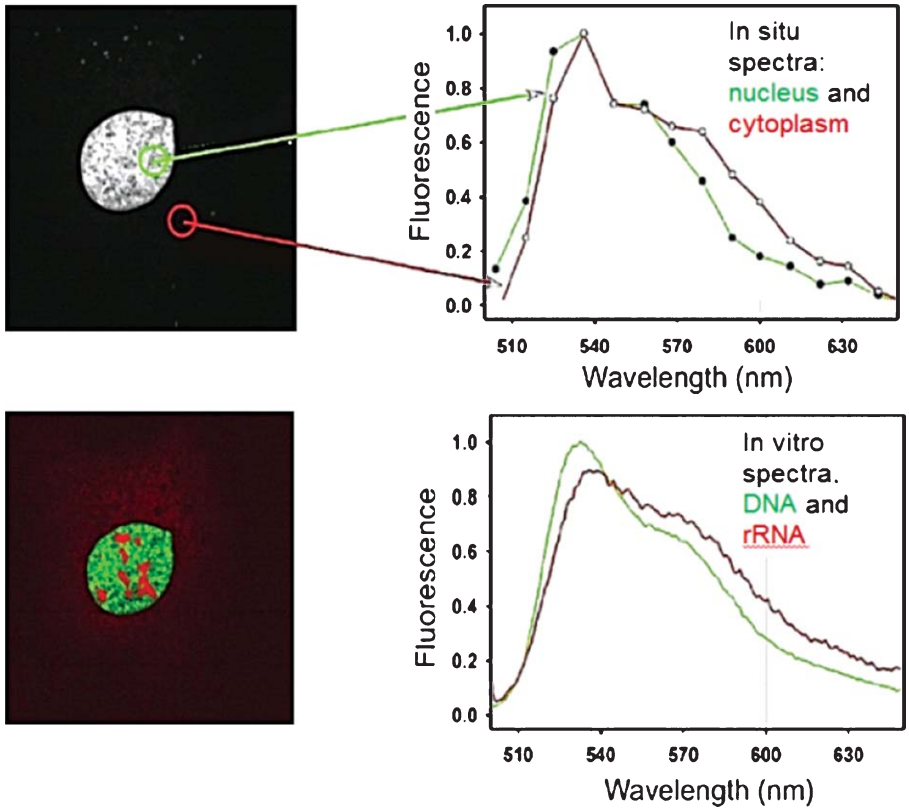

Fig. 4. Effects of nucleic acid binding on TOTO-1 spectra—detection of RNA-rich nuclear regions.

PSMA expression using a green quantum-dot-labeled antibody. The truly bright signals in the color image (top left) were due entirely to autofluorescence. Even a narrow bandpass filter centered on the peak, 535-nm emission of the quantum dot label (upper right panel) did not reveal the luminal distribution location of the PSMA molecules, which required spectral unmixing to demonstrate.

Spectra can reveal environmental effects on single dye emissions, as illustrated in Fig. 4, which shows how spectral imaging can be used in an exploratory mode. A cell was stained using the nucleic acid dye, TOTO-1, spectrally imaged on a confocal instrument, and spectra extracted from the nucleus (presumably reflecting largely DNA-binding events) and the cytoplasm (RNA and possibly minor contributions from mitochondrial DNA). Using these spectra, the image was unmixed (although classification would have given the same results) to delineate RNA-rich regions of the nucleus. The spectra taken from the cell were compared to spectra taken in solution when TOTO-1 was complexed with purified RNA and DNA; the similarities are evident.

Alternatively, autofluorescence arising from "interesting" endogenous molecules may also carry useful spectroscopic information. Autofluorescence spectra of, for example, NAD(P)H [53], flavins and flavoproteins [54], advanced glycation end-products (AGEs) [55], collagen and elastin [56], lipofuscins [57] and protoporphyrin IX [58] can provide insights into normal and pathological specimens [59, 60].

5.3. *Separation (also known as multiplexing)*

Being able to view multiple (molecular) signals simultaneously is one of the main attractions of spectral imaging. There are two main approaches. One is signal separation of multiple labels through spectral unmixing algorithms. The second may use unmixing as a first stage, but relies on bar-coding techniques to increase the number of distinguishable

entities, potentially by orders of magnitude. Both will be discussed in greater depth below.

5.4. Quantitation and analysis

Sensitive detection and accurate signal unmixing are prerequisites for valid quantitation of signal intensities and other objective measurements. If signal location and intensity cannot be determined precisely, all further computations may be suspect. Spectral imaging can convert semi-quantitative to quantitative assays, while improving lower limits of sensitivity (as shown in Figs. 2 and 3). It is consequently very important that spectral segmentation and/or unmixing be performed accurately, since errors at those steps will propagate; as with every complicated technique, the methods and algorithms must be validated and appropriate controls included [47].

Images with the location and intensities of the unmixed signals may be all that is necessary, since pictures may convey all the insights required. On the other hand, quantitation typically requires some spatial manipulations (identification of regions of interest, segmentation of nuclei, identification of subcellular compartments, etc.) and these may benefit from manual or automated image analysis tools, discussion of which is beyond the scope of this chapter. This is a rapidly evolving field; the new Journal of Pathology Informatics is a good source for recent publications.

6. Some spectral imaging hardware approaches

A tribute to human ingenuity is the fact that there are at least 10 or so quite different technology variants of spectral imaging, including filtered cameras (with a number of flavors), whiskbroom and pushbroom scanners, such as the Specim or PARISS systems [61, 62], multispectral laser confocal systems [63, 64], Fourier transform imaging spectrometers [65], computed tomography imaging spectrometers (CTIS) [66], image replicating imaging spectrometers (IRIS) [67, 68], coded aperture snapshot spectral imagers (CASSI) [69, 70], and snapshot spectral image slicing [71]—and that only covers emission-side spectroscopy [72–74]. Illumination light can also be be spectrally modulated to provide similar information [Frank, 2007 #7670, 75].

These methodologies capture spatial and spectral information using very different imaging geometries. Spatially, images can be acquired one point at a time (e.g., a confocal laser scanner), one line at a time, or a full frame at a time. The first case typically requires a laser spot scanning over a sample, the second requires either the sample or the optics to move, and the third typically requires no movement of either sample or imaging optics.

Spectrally, images can be acquired one wavelength at a time ("band-sequential"), or many wavelengths simultaneously—typically by diffracting the light so that the spectral information is dispersed along a collector, such as a multi-anode PMT or CCD. Airborne remote-sensing imaging systems typically utilize a line-scan approach, in which linear slices of the field are spectrally dispersed onto a 2-dimensional digital sensing array (a CCD or other device for detection outside of the visible region). This geometry has been adapted for use on the microscope by incorporating a scanning stage to move the slide underneath the detector (e.g., Specim or PARISS). An alternative way of collecting all wavelengths simultaneously involves Sagnac Fourier-transform interferometry [76], although this approach still requires the capture of multiple full-frame images and subsequent computation.

Finally, some approaches allow the collection of both spectral and spatial information simultaneously, and in a single acquisition ("snapshot"). These include computed tomographic imaging spectroscopy (CTIS) [66], or spectral image slicing [71], or simply arranging multiple spectrally filtered images onto single or multiple camera sensors, as in the Quad View product from Photometrics, or an intriguing variant that uses RGB sensors and custom color bandpasses [77].

The imaging slicing spectrometer has recently been commercialized by Rebellion Photonics, and can generate up to a 500 × 500-pixel image in as many as 200 spectral bands in a single snapshot with good light-capture efficiency. Frame-rates up to 100 frames per second are offered, along with real-time video-rate spectral unmixing. While simultaneously achieving high temporal, spectral and spatial resolution is a formidable challenge, it appears that this goal can be achieved. Nevertheless, at present, the most commonly used spectral imaging techniques are those found in confocal-based systems, the Sagnac Fourier-transform interferometer (ASI), and a variety of band-sequential

approaches such as those commercially available from CRI (now PerkinElmer) and Gooch & Housego.

Regardless of the hardware technology used, a spectral imager delivers three-dimensioned image sets (*x, y*, and wavelength intensity) that contain spectral information at every pixel. While "true" spectral imaging can deliver spectra containing hundreds or even thousands of spectrally distinct intensities at each pixel, such imaging *spectroscopy* is generally of less practical use than it might seem, depending on the task at hand. Capturing a subset of the available spectral information is usually sufficient and preferred—superfluous spectral data may simply increase statistical noise, processing time and storage requirements. Development of strategies for minimizing the amount of data collected while maximizing system performance remains an area of active research [78–80].

7. More on emission side band-sequential imaging

Band-sequential spectral imaging is one of the more straightforward techniques, since in its simplest form it can be accomplished simply by having a filter wheel containing multiple transmission filters (up to 20 in some systems) located in the optical train in front of the camera. The system takes a series of images while switching filters to create a spectral data stack. Large fields of view and/or high pixel resolution can be achieved with this approach. Flexibility can be achieved by having a many-position filter wheel, or the ability to swap in and out filters with different bandpass properties.

A particular advantage of this kind of imager is that the number of spectral bands acquired is completely up to the user, as opposed to techniques that collect continuous spectra, such as diffraction grating-based methods. Also, and importantly, dynamic range can be preserved, since different exposures can be employed at different wavelengths. This is helpful if, for example, a DAPI nuclear stain in the blue is extremely bright compared to a low-intensity fluorescent label in the green or red regions. Having the ability to take a very short exposure at 420 nm (blue) and a long exposure at 680 nm (red) allows both signals to be acquired with good signal-to-noise and without camera saturation. Disadvantages of filter-wheel methods include vibration, possible image shifts as different filters are rotated into the field of view, and bulky form-factors. Relatively slow switching speeds of the mechanical device can also dominate acquisition times and make it difficult to capture complete spectral stacks quickly enough to be practical for imaging transient phenomena and/or moving specimens. A variant of the filter-based approach synchronizes a rapidly and continuously spinning filter disk with a high-speed camera, allowing the capture of several multispectral images per second, as is possible with the SpectroCam from Ocean Thin Films.

Electronically tunable filters represent a promising alternative to mechanical filter wheels for a number of reasons. For one thing, there are no essential moving parts, and thus no noise or vibration is generated during wavelength switching. Secondly, the bandpasses are stable, compared to at least older-generation glass filters that could age or delaminate. Electronic filters can be randomly tuned, so that bands can be obtained in any order. This can be an advantage if some dyes need to be imaged first during data collection due to photostability issues. Also, with some technologies, transmission properties can be electronically altered to give control over the bandwidths and thus manipulate the trade-off between spectral resolution (the narrower the bandwidth, the higher the resolution) and light-capture efficiency (optimized with a large bandwidths). Disadvantages of most tunable filters include the fact that overall light throughput is less than that of traditional interference filters, by at least a factor of two (because typical tunable filters are polarization-sensitive, and, compared to interference filters, electronic filters usually have reduced out-of-band light rejection.

Two major tunable filter technologies are available: liquid crystal tunable filters (LCTFs) [81] and acousto-optical tunable filters (AOTFs) [16, 82]. Both of these have been incorporated into complete imaging systems ready for use on conventional microscopes via standard C-mounts, and are accompanied by capable software suites. Both technologies can acquire spectral datasets over similar wavelength ranges, and in both cases, separate filter models are required to address visible vs. near-infrared vs. mid-IR regions. In typical use, one would tune the filter to a desired wavelength, take a monochrome image, step the filter (often with a 10- or 20-nm interval), take another image, and so on. This process can be fully automated. The images are assembled into a spectral stack in the computer's memory and are available for immediate analysis, unlike other systems that may

require computationally intense iterative procedures to estimate spectral content. Well-designed tunable filters can offer diffraction-limited resolution, or even beyond; one recent reference described using surface plasmon particles imaged in dark field with 1-nm spectral resolution and 1.2 nm spatial resolution [83].

The time to acquire a complete stack depends strongly on a number of factors, most significantly on the number of wavelengths imaged, exposure times, filter-switching time, and camera-read-out rates. One major distinction between LCTF- and AOTF-based systems is filter-tuning speed. An LCTF typically can tune from one wavelength band to another in 50 to 75 *milli*seconds, whereas an AOTF can tune from band to band in about 50 *micro*seconds. When coupled with a fast camera, the AOTF's tuning speed opens up the possibility of near-real-time (i.e., video-rate) imaging in which complete spectral cubes (with a relatively small number of wavelengths) can be acquired, processed and displayed without significant visual lag. This of course requires that exposure times be short, but that can be the case in bright field imaging of chromogenically labeled specimens or with particularly bright fluorescent samples.

Another venerable tunable filter design, originated by C. Fabry and A. Perot back in 1899, is being revived by VTT (www.vtt.fi) with new optical coatings and inexpensive control hardware. With sub-millisecond tuning speed, up to 80% optical throughput and price points in the hundreds to low-thousands of dollars/euros per filter, Fabry-Perot technology may find its way into reasonably priced spectral imaging systems in the future.

8. Excitation- or illumination-side spectral Imaging

Wavelength control of fluorescence excitation sources or of bright field illumination offers some advantages over "camera-side" spectral filtering. For one thing, it is only the illumination path that is modulated, which leaves the optical path from sample to camera unaffected by additional optical elements such as tunable filters that can steal light and potentially affect image quality. Secondly, some illumination-side spectral sources can be tuned very rapidly, allowing for high-speed imaging. Finally, tuning the excitation source while capturing broadband emissions is essentially performing fluorescence excitation spectroscopy [84]; the resulting data can be used equivalently by spectral unmixing algorithms [85, 86].

Fluorescence illumination can also benefit significantly by being able to select and apply one or more illumination wavelengths perfectly matched to absorption maxima of different dyes. For wide-field fluorescence microscopy, there are a number of potential technologies to choose from. Monochromator-based light sources such as the Polychrome (Till Photonics), MEMS-based tunable sources such as those from OneLight or Gooch & Housego, and multi-LED solid-state light sources (e.g., Spectral X Light Engine, Lumencor; InsightSSI, Applied Precision; Colibri, Zeiss; Photofluor, 89 North; X-Cite LED1, Lumen Dynamics) enable rapid wavelength switching and selectable bandpasses. The same hardware facilitates rapid excitation switching to image eGFP, mCherry and other fluorescent proteins, including ratiometric fluorescent protein calcium sensors, pH, cAMP, and others.

Modern confocal microscopes are generally equipped with one or more lasers, with typical output being 405, 458, 476, 488, 514, 561, 592, and 633 nm. Thanks to the broadness of the excitation spectra of most fluorescent organic dyes and fluorescent proteins, most confocal microscopes have not needed excitation spectral tuning beyond that provided by multiple lasers to achieve useful separation of each fluorophore. The addition of tunable Ti:Sapphire lasers for generation of multiphoton fluorescence and second-harmonic and third-harmonic signals has added new capabilities to microscope imaging, and provides for additional excitation flexibility. Going further, some confocal microscopes are now equipped with supercontinuum white light lasers. Combined with wavelength selection (e.g., via AOTF or AOM control), this type of laser can deliver rapidly tunable fluorescence excitation at any wavelength over a wide spectral range.

9. Conventional filter cubes—still needed for multispectral imaging?

Fluorescence imaging requires that the very bright excitation light be excluded from the emission light path to avoid overpowering much weaker fluorescent emitted signals. Typically this is accomplished with sets of excitation and emission filters paired with appropriate dichroic mirrors that together block residual excitation light by as much as a million-

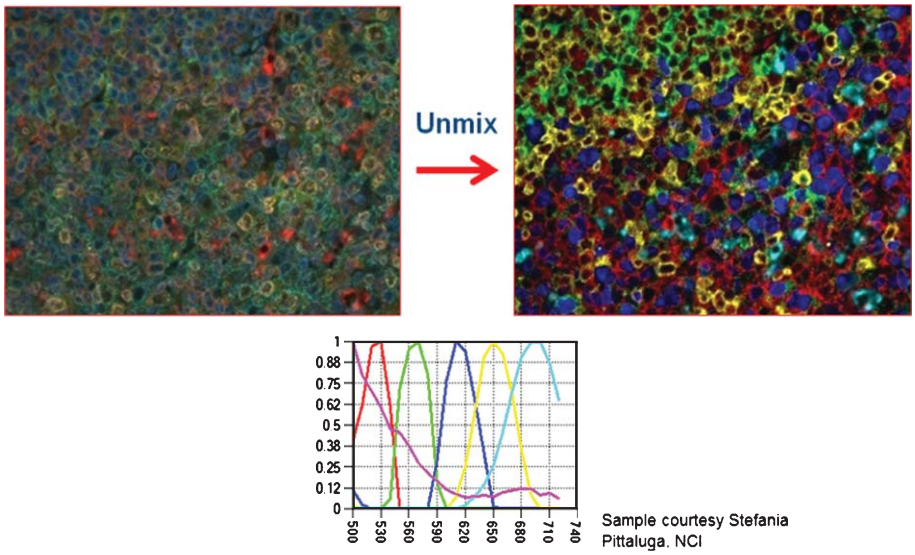

Fig. 5. Five quantum dots plus DAPI spectrally imaged, unmixed and displayed. The DAPI spectrum is shown, but the DAPI signal is not included in the composite image.

fold. Unfortunately, the tunable elements in many multispectral imaging systems only block out-of-band light by a factor of about 10,000-to-1, not sufficient to clean up all the unwanted excitation light. Consequently, a conventional interference filter is still required in front of the tunable optics to block excitation wavelengths. In any case, this is required for eye-safety with standard microscope configurations: most spectral imaging devices are connected to the microscope via a standard C-mount, and are thus "downstream" of the eyepieces. Without a standard emission filter in place to block excitation light, dangerous levels would be transmitted through the oculars and into the eyes of the microscope operator.

The advent of quantum dots reagents [38, 87–89] promised to simplify spectral imaging drastically, since quantum dots, regardless of emitted color, can be excited by wavelengths shorter than their emission peak. Thus, a single standard DAPI cube, for example, with a 500-nm longpass emission is able to excite and transmit all QD emitters from green to far-red with reasonable efficiency, as shown in Fig. 5.

Encouragingly, recent and intriguing developments in optical design suggest that full-range emission and excitation spectroscopy can be achieved without standard emission filters at all [90]—using polarization and structured illumination to reject out-of-band excitation light. These authors suggest that multispectral emission discrimination could be employed as a blocking strategy as well, and this was demonstrated by Gao et al. [91]. In the latter case, the authors suggest that a 3-fold improvement in signal-to-noise is achievable.

10. Other considerations

Other considerations for acquisition strategy include the selection of spectral range, spectral bandwidth (trading off spectral resolution with photon capture efficiency) and the total number of images to be acquired [92]. Clearly, one would like to use as small a spectral range and as few total image acquisitions as possible in order to cut down on imaging time, photobleaching and file size. In practice, however, when users start to use some commercial multispectral systems they may not stray from the default (full-range) settings for typical acquisitions, resulting in spectral datasets consisting of full-frame, full-resolution images from ∼400 to ∼700 nm with spectral steps every 10 or 20 nm, which is almost always surplus to requirement. The resulting bulky files and slower acquisition and analysis performance may induce new users to revert to imaging with more familiar, if less capable, conventional systems.

On the other hand, if the high-resolution spectral data is used initially to explore the spectral properties of specimens and labels, the information obtained can be used to optimize acquisition parameters for

multispectral or even conventional imaging approaches [93].

11. Image and spectral visualization, classification and unmixing

After a spectral data set is acquired, it is presented to the user, typically by mapping the series of spectral planes into a standard color (RGB) image that has nevertheless an optical spectrum associated with every pixel. The user can then use this image to help guide further analysis. Using the display tools in typical analysis software, one can "mouse" over the image and see a live spectrum associated with each pixel presented in another region of the screen. Mapping spectral information into an RGB image can be adjusted by changing which spectral ranges get combined to form the red, green and blue planes. Thus, fluorescent signals in the invisible, near-infrared region can be mapped into the red region, red-region intensities mapped to green, and so on.

Spectral image data sets can be remarkably rich in information and require appropriate (ideally, easy-to-use) techniques for analysis. The simplest tools are also some of the most useful, namely, straightforward *spectroscopy*, *classification* and *unmixing*. Supervised use of these tools requires the user to interact with a spectral library module that permits assignment of different spectra, typically via a series of colored (and name-able) buttons. By clicking on a colored box and then clicking or clicking-and-dragging in the display window over user-specified pixels particular spectral classes can be assembled, and their spectra shown in the spectrum display window. The spectral features usually are created by averaging the spectra from each selected pixel or area into a single, average spectrum, although some sophisticated analysis algorithms may utilize second- or higher order statistics [94]. The spectral library and display tools allow the user to directly compare spectra of different regions or objects and to download the spectra for further analysis. Spectra can also be stored and recalled for use in subsequent imaging sessions.

11.1. Spectroscopy

Fluorescent molecules can be sensitive to their environment, shifting excitation or emission properties.

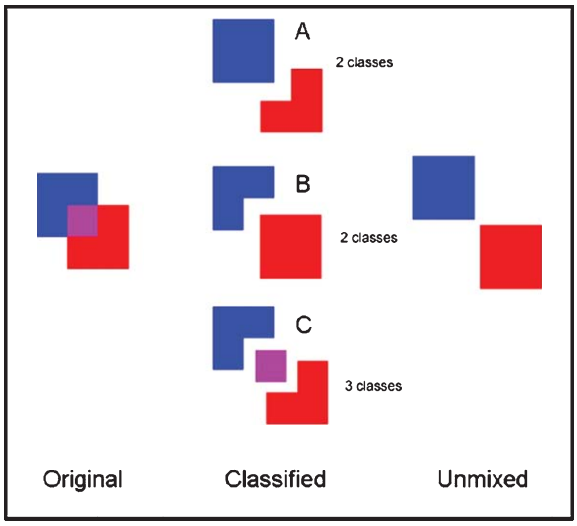

Fig. 6. Classification vs. unmixing.

This can either be a nuisance or a benefit, depending on the application. Consequently, one of the most useful and straightforward applications of spectral imaging is the measurement of the emission spectra of dyes *in situ*, rather than "*in cuvetto*," allowing for optimization of imaging parameters and increased understanding of the cellular milieu (Fig. 4). Other uses for spectroscopic-quality imaging include histology stain quality control and color normalization for digital imaging [95].

11.2. Classification

The distinction between classification and unmixing is illustrated in Fig. 6. The middle column shows the three possible outcomes of *classification*. Classification is equivalent to spectral segmentation; it is an exclusive operation in which a pixel or object is assigned to a single class. In this case one could use blue and red as the classes, and outcomes A or B might occur depending on whether the central purple region was more blue-like or red-like. Alternatively, 3 classes (red, blue and purple) could be used for classification, giving the result shown in outcome C. One might use this technique to segment nucleus from cytoplasm, since in theory, pixels in an image should belong to one or the other class (ignoring for the moment the problem of spatial overlap in thick samples). *Unmixing*, on the other hand, determines the abundance of blue and red at every pixel, and yields two separate images containing the blue signal and the red signal, in

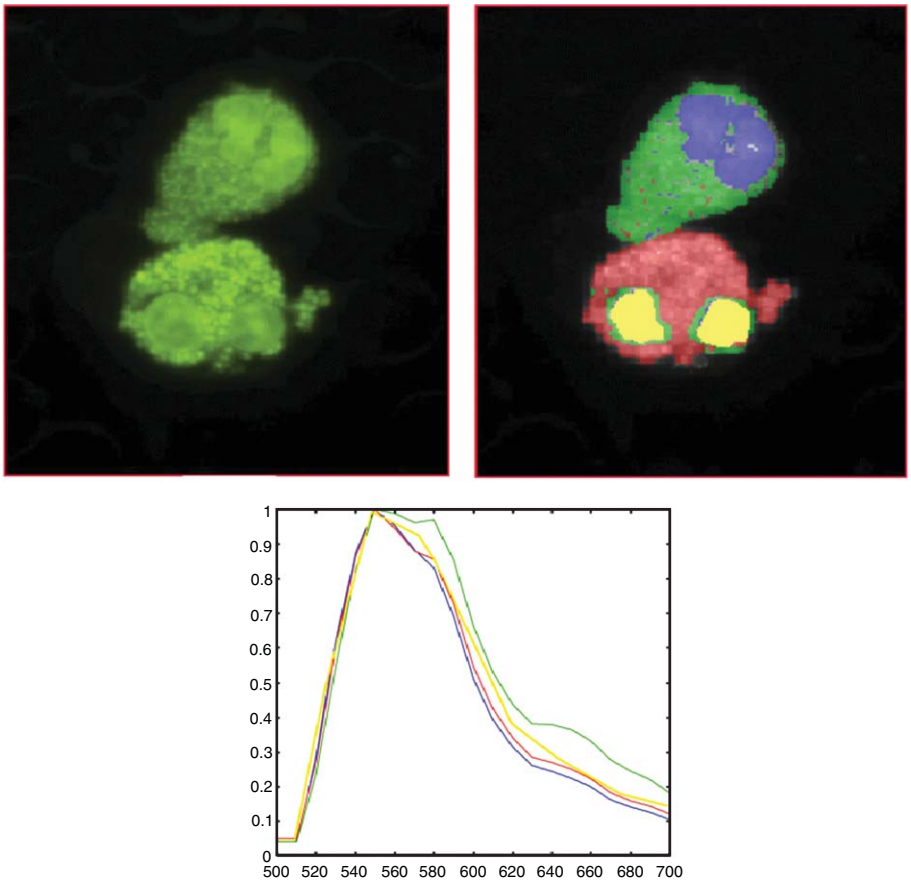

Fig. 7. Spectral classification of subcellular compartments in immature blood cells.

this case with uniform intensities regardless of whether the two signals spatially overlap (purple region) or not.

For classification, simple similarity metrics, such as Euclidean distance, can be used to compare the spectrum at each pixel with the set of classification spectra in the library, and then each pixel is assigned the class it most resembles. In Fig. 7, a pair of immature dog white blood cells were vitally stained with a single fluorescent dye, astrazone orange, and imaged using an LCTF-based instrument. Spectral classification tools (in this case, principal component analysis) could distinguish cytoplasmic and nuclear compartments from each other and moreover, distinguish the two types of cells (which represented different stages in white blood cell maturation). Examination of representative spectra from these 4 regions shows how subtle the spectral differences actually were. In this case, the spectra were combinations of the astrazone orange and fairly prominent cellular autofluorescence, which varied in the different cellular compartments.

The actual classification spectra used in the classification procedure can either be derived from the scene being analyzed or they can come from previously stored data. Alternatively, unsupervised or spatially constrained clustering methods can be used to explore and analyze multispectral images. These are complex solutions to difficult problems, typically found in the remote sensing field, and will not be further discussed. They may be, in fact, less useful than simple supervised techniques that can be applied to more predictable cellular or histological samples.

11.3. Unmixing

Unmixing, rather than classification, is the more common analytical tool used with multispectral

biomedical images. Overlapping signals in individual pixels will occur, for example, when labeled molecular targets occupy similar or closely adjacent cellular compartments, or when fluorescent signals are intermingled with autofluorescence. Thus, one must "unmix" the signals, typically using a model that treats the measured spectrum (at each pixel) as a linear mixture of 2 or more spectra [73]. A common variant relies on a constrained linear unmixing approach [16], which requires that there be only positive amounts of the various signals (since mathematically, it is possible to model the data using negative abundances) and which also ensures that the sum of all the class abundances reaches 100% (in other words, no allowance is made for the presence of unknown species in the sample). Unmixing fluorescently labeled images can become complicated or unreliable if there are multiple autofluorescent species, or if the fluorescent dyes are environmentally sensitive, and thus have varying spectra in different regions of a cell or tissue depending on local conditions. Also, the presence of non-linear interactions, such as energy transfer, between fluorescent species, such as energy transfer, will also introduce errors if the simple mixing model is being relied upon.

Linear unmixing software (as described in [96]) can unmix the data quickly and accurately. If preexisting measurements of the spectral properties of each component are available and assembled into spectral "libraries" for ready use, then the unmixing procedure requires no further interaction and can be accomplished in milliseconds, especially if the process is parallelized and/or ported for computations on graphical processing units (GPUs). Alternatively, appropriate spectra can be extracted from more complex, multiply stained samples using semi-automated spectral exploration software [40, 97]; generating accurate libraries normally takes just a few minutes, and once established, can be used on additional samples without further ado—as long as the samples are imaged on the same or similar instrument platforms.

Bright field imaging has certain advantages over fluorescence-based approaches because typically bright field data are converted from transmission units (what the camera natively "sees") to optical density (OD) units. Conversion to OD essentially makes the spectral data independent of typically encountered variables such as lamp intensity and color temperature, the transmission properties of any filters in the light path, and the spectral response of the camera. The conversion step typically involves dividing the sample spectral image by a corresponding blank (reference) image acquired (usually) from a clear area on a slide; this division effectively nulls out the effects of the variables listed above, while also helpfully flat-fielding the images. As a consequence, previously determined spectral libraries can regularly be used and even shared across institutions (as long as the reagents and their intrinsic spectra remain constant). Moreover, OD values directly reflect the abundance (absorbance) of the analytes in the specimen.

11.4. Display

After the unmixing step, the individual abundance images generated for each of the unmixed components can be combined into a "component" image containing all the unmixed species in one multiplane display and manipulated like "levels" in Photoshop. Individual components can be rendered visible or invisible as required, and can be re-colorized or otherwise adjusted for maximum visual clarity (Fig. 8). At the same time, the quantitative data from each of the unmixed components is available for analysis. Such data is essential for determining co-localization behavior, as simple Boolean operations, or more elaborated approaches, can be used to determine whether any pixel or anatomic structure is simultaneously positive for two or more markers.

When unmixing absorbing, chromogenically labeled samples, it is possible to display the unmixed results layered over a bright field background of just the hematoxylin (or even H&E) signal to mimic the appearance of conventional single-color stains. Additionally, one can re-color stains (for example, from brown to green) to enhance legibility. Similarly, it can be helpful to invert the color space and present the unmixing results in "pseudo-fluorescence"; sometimes having additive signals (in which red + green = brighter yellow, for example) against a black background can be a more useful viewing mode.

The converse is also true: fluorescence images can be inverted and re-colored to resemble bright field immunohistochemical preparations. These can be much easier to evaluate visually, not least because spatial context becomes more visible. This maneuver may make it more likely that fluorescence-enabled techniques will increasingly become part of the standard pathology tool chest. No matter what manipulations are used to enhance usability, it is important to recog-

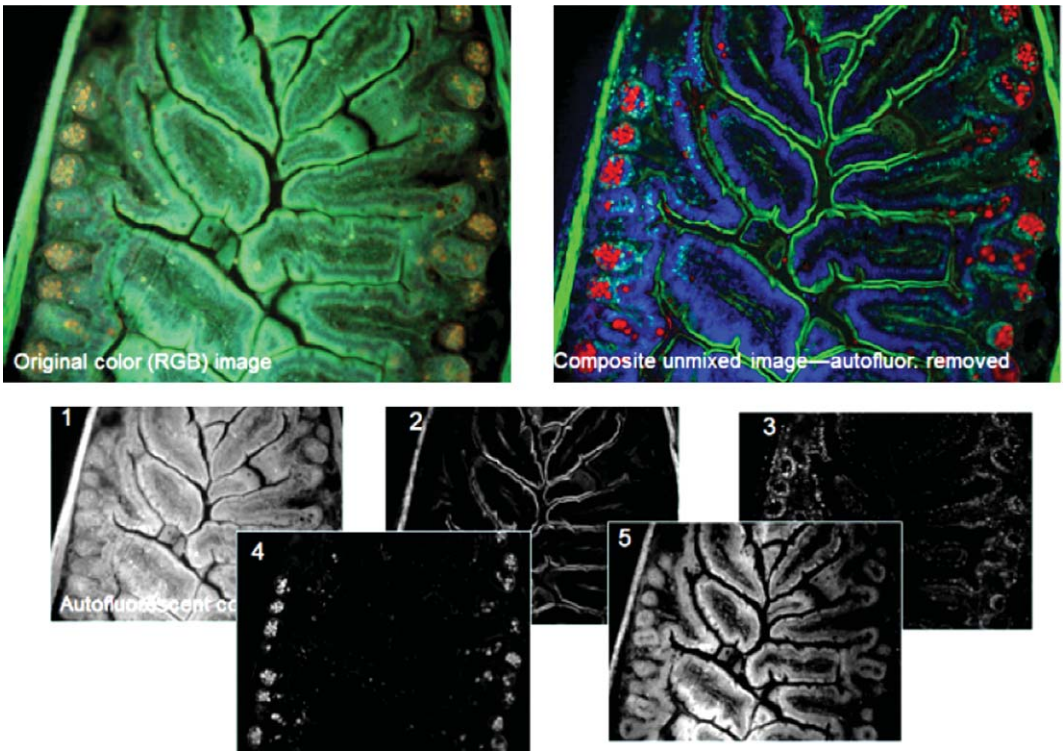

Fig. 8. Mouse bowel spectrally imaged. Four Alexa dyes and autofluorescence are unmixed; an AF-free composite is shown.

nize that these are just display options and do not affect the underlying quantitative data.

12. Bar-coding (combinatorial labeling)

Bar-coding, if technically feasible, offers up opportunities to resolve much greater sample complexity, and combines unmixing (to de-code the fluorescent label signal) followed by classification via look-up table. Barcoding works for samples that do not generally have different physical targets overlapping one another (unless the overlap can be depth-resolved optically, as with confocal microscopy), as it may otherwise be impossible to unambiguously assign a classification to areas of an image with mixed barcode signals. One of the first major applications of spectral imaging using this approach was spectral karyotyping (SKY) [98]. With over 900 citations in the 16 years since first published in 1996, SKY revolutionized mouse and human cytogenetics, and SKY probes have also been generated and applied to karyotyping non-human primates, rats and other species. SKY used combinatorial labeling of five fluorescent dyes (plus a DAPI counterstain for chromosome banding) and a simple on-off binary coding of chromosomes (i.e., On-off-off-off-off for chromosome 1, off-on-on-on-on for chromosome 24 (Y)) since the goal was to reach 24 human chromosomes with high confidence. The spatial constraint is that the method required cytogenetic chromosome spreads, ideally with no chromosome lying on top of another.

The Brainbow mouse [99] and its offshoots (so far, Drosophila, C. elegans, and Arabidopsis) have taken combinatorial labeling into the intact organism. By combining tissue/temporally inducible Cre recombinase, multiplex recombination sites encompassing multiple fluorescent protein gene cassettes, and spectral confocal microscopy, the inventors of the Brainbow mice report that by color and intensity over 90 different neuronal clones could be distinguished. Brainbow techniques could be further extended with additional colors, subcellular localization marking, fluorescent-protein-based Fucci cell cycle indicators [100], or

fluorescent protein biosensors, to increase information content per cell further.

Phenotyping of complex bacterial communities represents another intriguing application of bar-coding. In a proof of principle, Valm et al. employing RNA FISH and combinatorial labels were able to demonstrate 28 different binary combinations of eight fluorophores in visualizing *E. coli* in a model system [101]. Subsequently, they were able to image 15 taxa simultaneously in naturally occurring human dental plaque.

13. How many labels can be used simultaneously?

The answer to this, of course, is: it depends. The limits of conventional fluorescence-based multiplexing have not yet been fully explored, and will reflect the availability and quality of appropriate labels and ligands. Some of the factors that affect the degree of multiplexing that can be achieved, include the optics of the excitation and emission paths (one filter cube set or many?), the spectral properties and stability of the fluorophores, the brightness of the sample (dye brightness, amplification techniques, abundance of the targets, etc.), dynamic range, quantum efficiency and noise properties of the sensor, and the amount of confounding autofluorescence, and so on. A big factor affecting the degree of multiplexing possible is which general labeling technique is used—immunohistochemistry (perhaps 4 to 5) versus immunofluorescence ($\sim$10), for example.

A lack of suitable labeling techniques that can be readily employed without extensive in-house R& D has been an obstacle that has slowed down the adoption of spectral imaging. Traditional primary-secondary antibody tandem labeling techniques can be challenging to extend beyond 2 or 3 labels due to the difficulty of avoiding interference or cross-talk between the reagents, although a number of useful strategies have been developed to overcome these [102]. The development of advanced immunological labeling reagents (e.g., Zenon Technology from Life Technologies) allows the simultaneous use of several primary antibodies from the same species (e.g., mouse, rabbit, etc.) [103]. Multi-color plus multi-intensity multiplexing has also been documented using Zenon technology in the flow-cytometer [104].

Nevertheless, much detailed optimization is typically needed for each new set of reagents or targets, since fixation protocol, the order of antibody labeling, choice of labels, amplification systems, appropriate blocking, antibody dilution, antigen retrieval steps and so on can all affect the utility of staining results. Ideally, multiplexing should not interfere with sensitivity, specificity or quantitative relationships between antigens but it can happen that one antibody or chromogen label may physically block the subsequent labeling of the next antigen due to steric hindrance. In addition, attempting to combine various labels may run into problems of chemically incompatibility (e.g., trying to use both water- and alcohol-soluble chromogens). Finally, the use of multiple labels on a single specimen increases the demands for appropriate controls [105]. Fortunately, the advent of automated staining systems can relieve some of the logistical effort, at least, involved in multiplexed staining.

Some labeling strategies can facilitate multiplexing. For example, having available primary antibodies directly labeled with a variety of typical fluorescent dyes provides for simple protocols, but does not overcome the need for multiple excitation wavelengths to cover the spectral gamut. In the last few years, the situation has changed with the commercialization of quantum dot labels that can be used either with antibodies or molecular probes. Quantum dots are desirable in that a whole spectral variety of quantum dot labels, from the blue to the near-infrared, can be excited by a single source in the UV and deep blue, making for a simple optical set up [38, 106, 107]. Since the larger (i.e., redder) quantum dots are typically proportionately brighter than their smaller, bluer, versions, it can be important, as in most multiplexing situations, to ensure that the least abundant targets are tagged with the brightest labels, to intensity-balance the resulting signals as much as possible.

Some drawbacks of QDs continue to hinder their adoption. These include: a propensity to aggregate; blinking [108] (an attribute that can actually be used to enhance their detectability [109, 110]); and justifiable concerns about toxicity [111, 112], at least for the cadmium-selenium variety. Moreover, samples labeled with quantum dots *in vivo* and then processed for routine histology generally lose the quantum dot fluorescence. This effect was recently shown to be due to metal contaminants in most formaldehyde preparations, and with suitable care, QD introduced *in vivo* can still be detectable on subsequent histological sections [113].

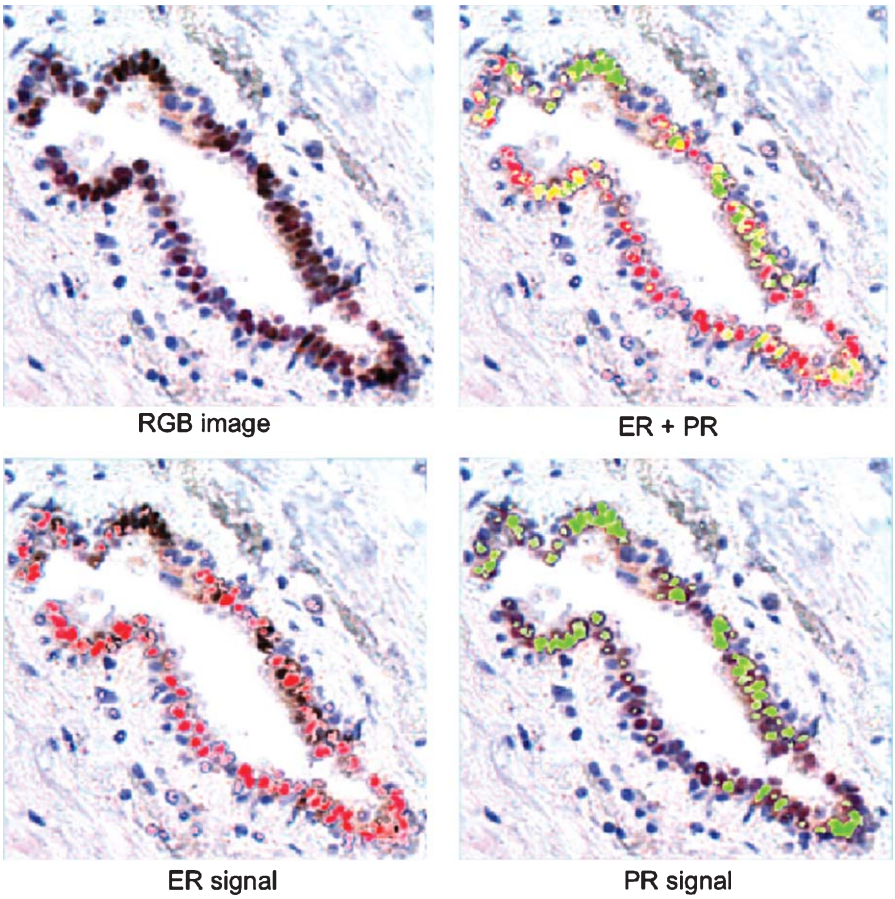

Fig. 9. Breast duct chromogenically stained for ER and PR, spectrally imaged in bright field and signals unmixed.

Recently a new class of multispectral dyes with certain advantages over quantum dots has been described [39]. These dyes are readily synthesized on conventional DNA synthesis machines and can be directly attached via "click"-chemistry to targeting moieties such as antibodies. Desirable properties include: very small size (∼1 nm); lack of toxic elements such as cadmium; and, like quantum dots, the capability of multispectral family members to be excited at one, near-UV wavelength region but to emit anywhere from blue to far-red.

In the case of bright field imaging, multiple chromogens of course exist for immunohistochemical staining. Fortunately, the common combination of DAB (brown), Fast Red (or the equivalent) for the molecular stains, and hematoxylin as the counterstain actually is quite well suited for spectral unmixing (Fig. 9). Getting past two or three chromogenic stains can be a challenge, but certain combinations of chromogens have been identified as being suitable for multiplexed spectral detection [102], and new chromogen combinations are being developed with this application specifically in mind. This will greatly enhance the use of simultaneous molecular stains for research and clinical pathology. While IHC-reagent suppliers have begun to develop multi-color IHC antibody- and chromogen panels (such as those, for example, available from BioCare Medical), their kits have largely employed labeling strategies that target different colors to non-spatially overlapping tissue elements (to avoid problems of color mixing that can make visual or standard digital color-based analyses difficult). If such companies develop application-specific kits that could take advantage of improved bright field

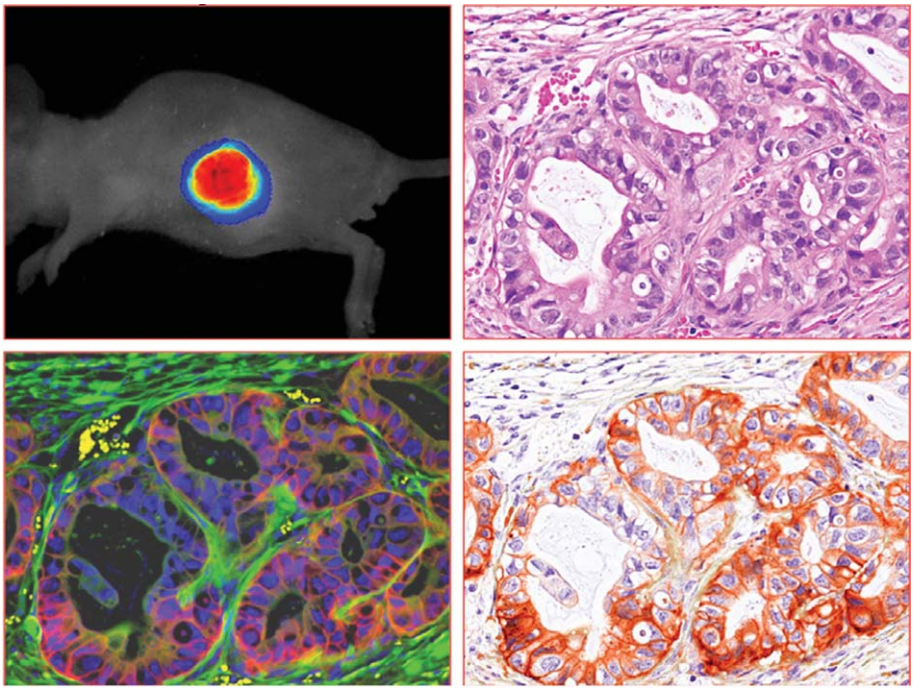

Fig. 10. Spectral imaging of fluorescent *in-vivo* molecular staining for HER2, H&E staining of FFPE tumor tissue, multispectral imaging, and color-space remapping.

signal separation, the usefulness and thus the use of spectral imaging in pathology would increase.

14. Going for 100-plex: alternatives to spectral imaging

Even with the advent of robust spectral image acquisition and analysis tools, spectral overlap can set upper limits on accuracy and dynamic range, and as the degree of multiplexing increases, so do the difficulties. The analogous situation in flow cytometry is illustrative. Flow cytometry has incrementally moved from one to as many as 18 fluorophores, plus forward and side scatter parameters. With just a few fluorophores in an assay, cross-talk compensation is readily achievable, but the modern (10+)-plex flow cytometer requires elaborate instrumentation, computer-controlled compensation and careful assay design [114].

A way to finesse the multiplexing problem is to do the labeling serially, rather than simultaneously. Serial staining, imaging, and "erasing" protocols can provide almost arbitrary degrees of multiplexing, although they can be slow and labor-intensive. Schubert and colleagues have achieved 50-plex and more by using just two colors, by staining, destaining (actually, photobleaching), and restaining through multiple cycles [115–117]. Using a related approach, Hennig and colleagues employed single-stranded DNA-conjugated antibodies, hybridizing with fluorescent oligonucleotides, then destaining using adjacent quencher oligonucleotides, and repeating, all at room temperature [118]. Currently, both these groups use pairs of fluorescent colors, but with spectral imaging approaches, this could be extended to four or more per cycle [119], increasing efficiency.

A recent publication [120] described a flow-based method that greatly exceeded the 20-plex flow barrier by switching from fluorescence to mass-encoded mass spectrometry, using the plasma-based CyTOF mass cytometer to measure the expression levels of 34 parameters per cell. The authors believe 60 and perhaps even 100 parameters can be measured simultaneously in using this method, at the rate of 1,000 cells per second. There are ways that this technology could eventually be extended to the analysis of solid tissues, although probably not with cellular-scale resolution.

15. Some additional developments and obstacles

The impact of whole-slide imaging in pathology may affect the adoption of multiplexed staining and analysis. The current models have become fast enough to support the conversion of pathology to a largely digital discipline [121]. Multispectral imaging can readily be adapted to at least some of these slide scanning technologies, and preliminary work has indicates that this combination will indeed be practical and useful. Having digital information for an entire specimen will allow for statistically valid quantitative tissue segmentation and quantitation techniques operating in a largely hands-off fashion. Pathologists would then perform a review and validation function, along with integration of slide imaging data with other sources of information as part of an overall clinical assessment [122]. As the imaging step no longer takes place on the pathologist's desk, it is now technically feasible to perform fluorescence-based staining, with its potential for enhanced multiplexing, while delivering a bright-field-like image to the pathologist, who ultimately may be unaware of the manner of slide preparing and imaging (see Fig. 10).

Q*uality control* still remains a big barrier. It is hard enough to maintain reproducible performance in histopathology laboratories using conventional staining methods, especially when antibodies are involved [123]. Molecular multiplexing will greatly increase the need for robust sample preparation and staining protocols and equally robust use of appropriate positive and negative controls, both qualitative and quantitative. Moreover, with multiple analytes, it is hard to come up with protocols, including antigen-retrieval steps, that will work with many protein targets simultaneously—formaldehyde is not the perfect fixative.

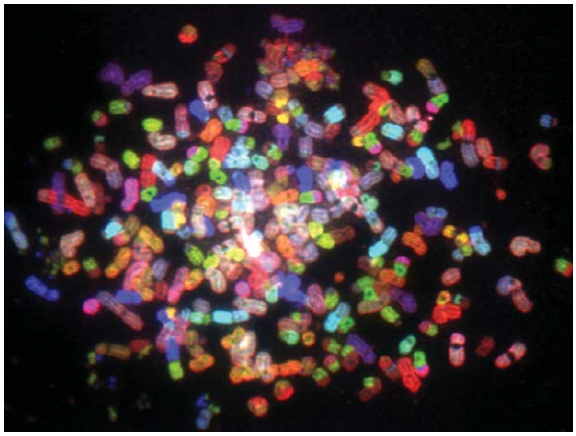

Fig. 11. Spectral karyotype of MDA-MB-435 single cell metaphase with 400 chromosomes. Each chromosome is pseudocolored based on a 5-dye spectral bar code.

Finally, computer-aided techniques carry the risk of user credulity: many people operating outside of their core expertise will accept computer-generated quantitative data uncritically, especially when it is difficult or impossible to confirm the results by eye. The use of computerized approaches must be therefore be accompanied by appropriate training and skepticism [124].

16. Summary

The era of spectrally resolved microscopy is still just beginning, with new and more affordable devices working in both wide field and confocal modes. The challenge has now shifted from the optical engineering phase to the development of robust and easy-to-use acquisition, analysis and presentation software tools, and equally importantly, the parallel development of new and existing dyes and dye (and chromogen) combinations. We anticipate staining methods employing possibly 10's of spectrally and spatially resolvable cell or tissue-based targets will becoming feasible in the near future, providing information simultaneously on the morphological, molecular and metabolic status of cells and tissues. Spectral imaging's ability to detect multiple analytes in unhomogenized, spatially intact, and possibly scanty specimens at subcellular resolution can provide information unavailable from other molecular profiling approaches such as expression arrays, targeted or deep sequencing, serum proteomics or *in-vivo* molecular imaging.

Despite the potential advantages that spectral imaging has to offer over ensemble-averaged molecular assays and conventional microscopy image capture, it still remains confined largely to the basic science domain and has not been widely adopted in clinical research, much less in clinical practice. This is a pity, since robust multiplexed imaging can provide pathology with many of the tools needed to refine prognosis, guide therapy selection and monitor ongoing therapeutic response. One can hope that the recent advances in multispectral hardware, software, and reagents will lead to better understanding of disease and better care of patients.

References

[1] W.A. Wells, P.E. Barker, C. MacAulay, M. Novelli, R.M. Levenson and J.M. Crawford, Validation of novel optical imaging technologies: The pathologists' view, *J Biomed Opt* **12** (2007), 051801.

[2] M.E. van den Akker-van Marle, D. Gurwitz, S.B. Detmar, C.M. Enzing, M.M. Hopkins, E. Gutierrez de Mesa and D. Ibarreta, Cost-effectiveness of pharmacogenomics in clinical practice: A case study of thiopurine methyltransferase genotyping in acute lymphoblastic leukemia in Europe, *Pharmacogenomics* **7** (2006), 783–792.

[3] M. Titford, The long history of hematoxylin, *Biotech Histochem* **80** (2005), 73–78.

[4] R.E. Heller, A requiem for aniline dyes, *Perspect Biol Med* **35** (1992), 398–400.

[5] C.R. Taylor and R.J. Cote, Immunohistochemical markers of prognostic value in surgical pathology, *Histol Histopathol* **12** (1997), 1039–1055.

[6] S.S. Bacus, D.A. Altomare, L. Lyass, D.M. Chin, M.P. Farrell, K. Gurova, A. Gudkov and J.R. Testa, AKT2 is frequently upregulated in HER-2/neu-positive breast cancers and may contribute to tumor aggressiveness by enhancing cell survival, *Oncogene* **21** (2002), 3532–3540.

[7] R.K. Reddy, C. Mao, P. Baumeister, R.C. Austin, R.J. Kaufman and A.S. Lee, Endoplasmic reticulum chaperone protein GRP78 protects cells from apoptosis induced by topoisomerase inhibitors: Role of ATP binding site in suppression of caspase-7 activation, *J Biol Chem* **278** (2003), 20915–20924.

[8] J. Cicenas, P. Urban, W. Kung, V. Vuaroqueaux, M. Labuhn, E. Wight, U. Eppenberger and S. Eppenberger-Castori, Phosphorylation of tyrosine 1248-ERBB2 measured by chemiluminescence-linked immunoassay is an independent predictor of poor prognosis in primary breast cancer patients, *Eur J Cancer* **42** (2006), 636–645.

[9] O. David, J. Jett, H. LeBeau, G. Dy, J. Hughes, M. Friedman and A.R. Brody, Phospho-Akt overexpression in non-small cell lung cancer confers significant stage-independent survival disadvantage, *Clin Cancer Res* **10** (2004), 6865–6871.

[10] E. Tokunaga, Y. Kimura, E. Oki, N. Ueda, M. Futatsugi, K. Mashino, M. Yamamoto, M. Ikebe, Y. Kakeji, H. Baba and Y. Maehara, Akt is frequently activated in HER2/neu-positive breast cancers and associated with poor prognosis among hormone-treated patients, *Int J Cancer* **118** (2006), 284–289.

[11] A. Lugli, I. Zlobec, P. Minoo, K. Baker, L. Tornillo, L. Terracciano and J.R. Jass, Role of the mitogen-activated protein kinase and phosphoinositide 3-kinase/AKT pathways downstream molecules, phosphorylated extracellular signal-regulated kinase, and phosphorylated AKT in colorectal cancer-a tissue microarray-based approach, *Hum Pathol* **37** (2006), 1022–1031.

[12] S.B. Vestey, C. Sen, C.J. Calder, C.M. Perks, M. Pignatelli and Z.E. Winters, Activated Akt expression in breast cancer: Correlation with p53, Hdm2 and patient outcome, *Eur J Cancer* **41** (2005), 1017–1025.

[13] S. Yamamoto, Y. Tomita, Y. Hoshida, T. Morooka, H. Nagano, K. Dono, K. Umeshita, M. Sakon, O. Ishikawa, H. Ohigashi, S. Nakamori, M. Monden and K. Aozasa, Prognostic significance of activated Akt expression in pancreatic ductal adenocarcinoma, *Clin Cancer Res* **10** (2004), 2846–2850.

[14] J. Luo, B.D. Manning and L.C. Cantley, Targeting the PI3K-Akt pathway in human cancer: Rationale and promise, *Cancer Cell* **4** (2003), 257–262.

[15] J. Bergqvist, G. Elmberger, J. Ohd, B. Linderholm, J. Bjohle, H. Hellborg, H. Nordgren, A.L. Borg, L. Skoog and J. Bergh, Activated, ERK1/2 and phosphorylated oestrogen receptor alpha are associated with improved breast cancer survival in women treated with tamoxifen, *Eur J Cancer* **42** (2006), 1104–1112.

[16] R.M. Levenson, E.S. Wachman, W. Niu and D.L. Farkas, Spectral imaging in biomedicine: A selective overview, *Proc SPIE* **3438** (1998), 300–312.

[17] M.P. DiGiovanna and D.F. Stern, Activation state-specific monoclonal antibody detects tyrosine phosphorylated p185neu/erbB-2 in a subset of human breast tumors overexpressing this receptor, *Cancer Res* **55** (1995), 1946–1955.

[18] B.Z. Ring, R.S. Seitz, R. Beck, W.J. Shasteen, S.M. Tarr, M.C. Cheang, B.J. Yoder, G.T. Budd, T.O. Nielsen, D.G. Hicks, N.C. Estopinal and D.T. Ross, Novel prognostic immunohistochemical biomarker panel for estrogen receptor-positive breast cancer, *J Clin Oncol* **24** (2006), 3039–3047.

[19] D. Loussouarn, J. Brunon, H. Avet-Loiseau, M. Campone and J.F. Mosnier, Prognostic value of HER2 expression in meningiomas: An immunohistochemical and fluorescence *in situ* hybridization study, *Hum Pathol* **37** (2006), 415–421.

[20] S.M. Wiseman, N. Makretsov, T.O. Nielsen, B. Gilks, E. Yorida, M. Cheang, D. Turbin, K. Gelmon and D.G. Huntsman, Coexpression of the type 1 growth factor receptor family members HER-1, HER-2, and HER-3 has a synergistic negative prognostic effect on breast carcinoma survival, *Cancer* **103** (2005), 1770–1777.

[21] G. Jayaram and E.M. Elsayed, Cytologic evaluation of prognostic markers in breast carcinoma, *Acta Cytol* **49** (2005), 605–610.

[22] N.A. Makretsov, D.G. Huntsman, T.O. Nielsen, E. Yorida, M. Peacock, M.C.U. Cheang, S.E. Dunn, M. Hayes, M. van de Rijn, C. Bajdik and C.B. Gilks, Hierarchical clustering analysis of tissue microarray immunostaining data identifies prognostically significant groups of breast carcinoma, *Clin Cancer Res* **10** (2004), 6143–6151.

[23] S. Abdul-Rasool, S.H. Kidson, E. Panieri, D. Dent, K. Pillay and G.S. Hanekom, An evaluation of molecular markers for improved detection of breast cancer metastases in sentinel nodes, *J Clin Pathol* **59** (2006), 289–297.

[24] W. Pao and N. Girard, New driver mutations in non-small-cell lung cancer, *The Lancet Oncology* **12** (2011), 175–180.

[25] P.T. Nelson, D.A. Baldwin, W.P. Kloosterman, S. Kauppinen, R.H. Plasterk and Z. Mourelatos, RAKE and LNA-ISH reveal microRNA expression and localization in archival human brain, *RNA* **12** (2006), 187–191.

[26] P.T. Nelson, M. De Planell-Saguer, S. Lamprinaki, M. Kiriakidou, P. Zhang, U. O'Doherty and Z. Mourelatos, A novel monoclonal antibody against human Argonaute proteins reveals unexpected characteristics of miRNAs in human blood cells, *RNA* **13** (2007), 1787–1792.

[27] S.S. Jeffrey, Cancer biomarker profiling with microRNAs, *Nat Biotechnol* **26** (2008), 400–401.

[28] N.L. Simone, R.F. Bonner, J.W. Gillespie, M.R. Emmert-Buck and L.A. Liotta, Laser-capture microdissection: Opening the microscopic frontier to molecular analysis, *Trends Genet* **14** (1998), 272–276.
[29] J.M. Lubieniecka and T.O., Nielsen, cDNA microarray-based translational research in soft tissue sarcoma, *Journal of Surgical Oncology* **92** (2005), 267–271.
[30] R.E. Banks, M.J. Dunn, M.A. Forbes, A. Stanley, D. Pappin, T. Naven, M. Gough, P. Harnden and P.J. Selby, The potential use of laser capture microdissection to selectively obtain distinct populations of cells for proteomic analysis– preliminary findings, *Electrophoresis* **20** (1999), 689–700.
[31] F. Fend, M.R. Emmert-Buck, R. Chuaqui, K. Cole, J. Lee, L.A. Liotta and M. Raffeld, Immuno-LCM: Laser capture microdissection of immunostained frozen sections for mRNA analysis, *Am J Pathol* **154** (1999), 61–66.
[32] J. Liu, S.K. Lau, V.A. Varma, B.A. Kairdolf and S. Nie, Multiplexed detection and characterization of rare tumor cells in Hodgkin's lymphoma with multicolor quantum dots, *Anal Chem* **82** (2010), 6237–6243.
[33] M.H. Oktay, F.B. Gertler, Y.F. Liu, T.E. Rohan, J.S. Condeelis and J.G. Jones, Correlated immunohistochemical and cytological assays for the prediction of hematogenous dissemination of breast cancer, *J Histochem Cytochem* **60** (2012), 168–173.
[34] W.J. Frable, Pathologic classification of soft tissue sarcomas, *Semin Surg Oncol* **10** (1994), 332–339.
[35] Z.H. Zhu, B.Y. Sun, Y. Ma, J.Y. Shao, H. Long, X. Zhang, J.H. Fu, L.J. Zhang, X.D. Su, Q.L. Wu, P. Ling, M. Chen, Z.M. Xie, Y. Hu and T.H. Rong, Three immunomarker support vector machines-based prognostic classifiers for stage IB non-small-cell lung cancer, *J Clin Oncol* **27** (2009), 1091–1099.
[36] M.A. Rubin, M.P. Zerkowski, R.L. Camp, R. Kuefer, M.D. Hofer, A.M. Chinnaiyan and D.L. Rimm, Quantitative determination of expression of the prostate cancer protein alpha-methylacyl-CoA racemase using automated quantitative analysis (AQUA): A novel paradigm for automated and continuous biomarker measurements, *Am J Pathol* **164** (2004), 831–840.
[37] T.J. Fountaine, S.M. Wincovitch, D.H. Geho, S.H. Garfield and S. Pittaluga, Multispectral imaging of clinically relevant cellular targets in tonsil and lymphoid tissue using semiconductor quantum dots, *Mod Pathol* **19** (2006), 1181–1191.
[38] R.J. Byers and E.R. Hitchman, Quantum dots brighten biological imaging, *Prog Histochem Cytochem* **45** (2011), 201–237.
[39] J. Guo, S. Wang, N. Dai, Y.N. Teo and E.T. Kool, Multispectral labeling of antibodies with polyfluorophores on a DNA backbone and application in cellular imaging, *Proc Natl Acad Sci U S A* **108** (2011), 3493–3498.
[40] J.R. Mansfield, K.W. Gossage, C.C. Hoyt and R.M. Levenson, Autofluorescence removal, multiplexing, and automated analysis methods for *in-vivo* fluorescence imaging, *J Biomed Opt* **10** (2005), 41207.
[41] R.M. Levenson and J.R. Mansfield, Multispectral imaging in biology and medicine: Slices of life, *Cytometry A* **69** (2006), 748–758.
[42] B. Clancy and L.J. Cauller, Reduction of background autofluorescence in brain sections following immersion in sodium borohydride, *J Neurosci Methods* **83** (1998), 97–102.
[43] W. Baschong, R. Suetterlin and R.H. Laeng, Control of autofluorescence of archival formaldehyde-fixed, paraffin-embedded tissue in confocal laser scanning microscopy (CLSM), *J Histochem Cytochem* **49** (2001), 1565–1572.
[44] T.J. Staughton, C.J. McGillicuddy and P.D. Weinberg, Techniques for reducing the interfering effects of autofluorescence in fluorescence microscopy: Improved detection of sulphorhodamine B-labelled albumin in arterial tissue, *J Microsc* **201** (2001), 70–76.
[45] M. Neumann and D. Gabel, Simple method for reduction of autofluorescence in fluorescence microscopy, *J Histochem Cytochem* **50** (2002), 437–439.
[46] P.C. Roche, V.J. Suman, R.B. Jenkins, N.E. Davidson, S. Martino, P.A. Kaufman, F.K. Addo, B. Murphy, J.N. Ingle and E.A. Perez, Concordance between local and central laboratory HER2 testing in the breast intergroup trial N9831, *J Natl Cancer Inst* **94** (2002), 855–857.
[47] C.R. Taylor and R.M. Levenson, Quantification of immunohistochemistry–issues concerning methods, utility and semiquantitative assessment II, *Histopathology* **49** (2006), 411–424.
[48] W.J. Cukierski and D.J. Foran, Metamerism in Multispectral Imaging of Histopathology Specimens. *Proceedings/IEEE International Symposium on Biomedical Imaging: From nano to macro, IEEE International Symposium on Biomedical Imaging* **2010** (2010), 145–148.
[49] M. Speicher, S. Gwyn Ballard and D. Ward, Karyotyping human chromosomes by combinatorial multi-fluor FISH, *Nat Genet* **12** (1996), 368–375.
[50] J.A. Kiernan, Suppressing autofluorescence, *Biotech Histochem* **77** (2002), 232.
[51] R. Levenson, P.J. Cronin and K.P. Pankratov, Spectral imaging for brightfield microscopy, *Proc SPIE* **4959** (2003), 27–33.
[52] R. Levenson, Putting the "more" back in morphology: Spectral imaging and image analysis in the service of pathology, *Arch Pathol Lab Med* **132** (2008), 748–757.
[53] S. Villette, S. Pigaglio-Deshayes, C. Vever-Bizet, P. Validire and G. Bourg-Heckly, Ultraviolet-induced autofluorescence characterization of normal and tumoral esophageal epithelium cells with quantitation of NAD(P)H, *Photochem Photobiol Sci* **5** (2006), 483–492.
[54] D. Chorvat, Jr., J. Kirchnerova, M. Cagalinec, J. Smolka, A. Mateasik and A. Chorvatova, Spectral unmixing of flavin autofluorescence components in cardiac myocytes, *Biophys J* **89** (2005), L55–L57.
[55] A.A. Ghazaryan, P.S. Hu, S.J. Chen, H.Y. Tan and C.Y. Dong, Spatial and temporal analysis of skin glycation by the use of multiphoton microscopy and spectroscopy, *J Dermatol Sci*, 2011.
[56] B. Lin, M.S. Bergholt, D.P. Lau and Z. Huang, Diagnosis of early stage nasopharyngeal carcinoma using ultraviolet autofluorescence excitation-emission matrix spectroscopy and parallel factor analysis, *Analyst* **136** (2011), 3896–3903.
[57] R.S. DaCosta, H. Andersson, M. Cirocco, N.E. Marcon and B.C. Wilson, Autofluorescence characterisation of isolated

whole crypts and primary cultured human epithelial cells from normal, hyperplastic, and adenomatous colonic mucosa, *J Clin Pathol* **58** (2005), 766–774.
[58] B.H. Li and S.S. Xie, Autofluorescence excitation-emission matrices for diagnosis of colonic cancer, *World J Gastroenterol* **11** (2005), 3931–3934.
[59] M. Monici, G. Agati, F. Fusi, R. Pratesi, M. Paglierani, V. Santini and P.A. Bernabei, Dependence of leukemic cell autofluorescence patterns on the degree of differentiation, *Photochem Photobiol Sci* **2** (2003), 981–987.
[60] M. Monici, V. Basile, G. Romano, L. Evangelisti, L. Lucarini, M. Attanasio, E. Bertini, F. Fusi, G.F. Gensini, G. Pepe, Fibroblast autofluorescence in connective tissue disorders: A future tool for clinical and differential diagnosis? *Journal of Biomedical Optics* **13** (2008), 054025.
[61] A. Del Fiore, M. Reverberi, A. Ricelli, F. Pinzari, S. Serranti, A.A. Fabbri, G. Bonifazi and C. Fanelli, Early detection of toxigenic fungi on maize by hyperspectral imaging analysis, *International Journal of Food Microbiology* **144** (2010), 64–71.
[62] J.M. Lerner, N. Gat, E. Wachman, Approaches to spectral imaging hardware, *Current Protocols in Cytometry/Editorial Board, J. Paul Robinson, managing Editor... [et al.]* **Chapter 12** (2010), Unit 12 20.
[63] M.E. Dickinson, G. Bearman, S. Tille, R. Lansford, S.E. Fraser, Multi-spectral imaging and linear unmixing add a whole new dimension to laser scanning fluorescence microscopy, *Biotechniques* **31** (2001), 1272, 1274-1276, 1278.
[64] B. Rajwa, Modern confocal microscopy, *Current Protocols in Cytometry/Editorial Board, J. Paul Robinson, managing Editor... [et al.]* **Chapter 12** (2005), Unit 12 3.
[65] Z. Malik, M. Dishi and Y. Garini, Fourier transform multipixel spectroscopy and spectral imaging of protoporphyrin in single melanoma cells, *Photochem. Photobiol* **63** (1996), 608–614.
[66] B.K. Ford, C.E. Volin, S.M. Murphy, R.M. Lynch and M.R. Descour, Computed tomography-based spectral imaging for fluorescence microscopy, *Biophys J* **80** (2001), 986–993.
[67] A. Gorman, D.W. Fletcher-Holmes and A.R. Harvey, Generalization of the Lyot filter and its application to snapshot spectral imaging, *Optics express* **18** (2010), 5602–5608.
[68] D.J. Mordant, I. Al-Abboud, G. Muyo, A. Gorman, A. Sallam, P. Ritchie, A.R. Harvey and A.I. McNaught, Spectral imaging of the retina, *Eye* **25** (2011), 309–320.
[69] A.A. Wagadarikar, N.P. Pitsianis, X. Sun and D.J. Brady, Video rate spectral imaging using a coded aperture snapshot spectral imager, *Optics express* **17** (2009), 6368–6388.
[70] C.F. Cull, K. Choi, D.J. Brady and T. Oliver, Identification of fluorescent beads using a coded aperture snapshot spectral imager, *Applied optics* **49** (2010), B59–B70.
[71] L. Gao, R.T. Kester, N. Hagen and T.S. Tkaczyk, Snapshot Image Mapping, Spectrometer, (IMS) with high sampling density for hyperspectral microscopy, *Optics express* **18** (2010), 14330–14344.
[72] C.D. Tran, Development and analytical applications of multispectral imaging techniques: An overview, *Fresenius J Anal Chem* **369** (2001), 313–319.
[73] Y. Hiraoka, T. Shimi and T. Haraguchi, Multispectral imaging fluorescence microscopy for living cells, *Cell Struct Funct* **27** (2002), 367–374.
[74] G. Bearman, R. Levenson, Biological Imaging Spectroscopy, In: *Biomedical Photonics Handbook*, T. Vo-Dinh, Editor, CRC Press, Boca Raton, (2003), p. 8_1-8_26.
[75] M.M. Schulz, F. Wehner and H.D. Wehner, The use of a tunable light source (Mini-Crimescope MCS-400, SPEX Forensics) in dissecting microscopic detection of cryptic epithelial particles, *Journal of forensic sciences* **52** (2007), 879–883.
[76] Y. Garini, N. Katzir, D. Cabib, R.A. Buckwald, D.G. Soenksen, Z. Malik, Spectral Bio-Imaging, In: *Fluorescence Imaging Spectroscopy and Microscopy*, X.F. Wang and B. Herman, Editors., John Wiley & Sons, Inc., 1996.
[77] G. Themelis, J.S. Yoo and V. Ntziachristos, Multispectral imaging using multiple-bandpass filters, *Optics letters* **33** (2008), 1023–1025.
[78] R. Neher and E. Neher, Optimizing imaging parameters for the separation of multiple labels in a fluorescence image, *Journal of Microscopy* **213** (2004), 46–62.
[79] T.C. Wood, S. Thiemjarus, K.R. Koh, D.S. Elson, G.Z. Yang, Optimal feature selection applied to multispectral fluorescence imaging, in: *Medical image computing and computer-assisted intervention (MICCAI)*, London, 2008.
[80] J. Minet, J. Taboury, F. Goudail, M. Péalat, N. Roux, J. Lonny and Y. Ferrec, Influence of band selection and target estimation error on the performance of the matched filter in hyperspectral imaging, *Applied Optics* **50** (2011), 4276–4285.
[81] C. Hoyt, Liquid crystal tunable filters clear the way for imaging multiprobe fluorescence, *Biophotonics International* July/August (1996), 49–51.
[82] E.S. Wachman, W. Niu and D.L. Farkas, AOTF microscope for imaging with increased speed and spectral versatility, *Biophysical Journal* **73** (1997), 1215–1222.
[83] T. Huang, L.M. Browning and X.H. Xu, Far-field photostable optical nanoscopy (PHOTON) for real-time super-resolution single-molecular imaging of signaling pathways of single live cells, *Nanoscale*, 2012.
[84] A.J. Chaudhari, S. Ahn, R. Levenson, R.D. Badawi, S.R. Cherry and R.M. Leahy, Excitation spectroscopy in multispectral optical fluorescence tomography: Methodology, feasibility and computer simulation studies, *Physics in Medicine and Biology* **54** (2009), 4687–4704.
[85] C. Dunsby, P.M.P. Lanigan, J. McGinty, D.S. Elson, J. Requejo-Isidro, I. Munro, N. Galletly, F. McCann, B. Treanor, B. Önfelt, D.M. Davis, M.A.A. Neil and P.M.W. French, An electronically tunable ultrafast laser source applied to fluorescence imaging and fluorescence lifetime imaging microscopy, *Journal of Physics D: Applied Physics* **37** (2004), 3296.
[86] K.R. Koh, T. Wood, H. Zhang, K. Lekadir, D. Elson, G.-Z. Yang, Fluorescence excitation spectroscopic imaging with a tuneable light source and dimensionality reduction using FR-IsoMap, *Proc SPIE* **6848** (2008), 68480Z-1-8.
[87] W.C. Chan and S. Nie, Quantum dot bioconjugates for ultrasensitive nonisotopic detection, *Science* **281** (1998), 2016–2018.

[88] T.D. Lacoste, X. Michalet, F. Pinaud, D.S. Chemla, A.P. Alivisatos and S. Weiss, Ultrahigh-resolution multicolor colocalization of single fluorescent probes, *Proc Natl Acad Sci U S A* **97** (2000), 9461–9466.

[89] J. Itoh and R.Y. Osamura, Quantum dots for multicolor tumor pathology and multispectral imaging, *Methods Mol Biol* **374** (2007), 29–42.

[90] M.J. Booth, A. Jesacher, R. Juskaitis and T. Wilson, Full spectrum filterless fluorescence microscopy, *Journal of microscopy* **237** (2010), 103–109.

[91] L. Gao, N. Hagen and T.S. Tkaczyk, Quantitative comparison between full-spectrum and filter-based imaging in hyperspectral fluorescence microscopy, *J Microsc*, 2012.

[92] A. Mazhar, S. Dell, D.J. Cuccia, S. Gioux, A.J. Durkin, J.V. Frangioni and B.J. Tromberg, Wavelength optimization for rapid chromophore mapping using spatial frequency domain imaging, *Journal of Biomedical Optics* **15** (2010), 061716.

[93] I.B. Styles, Selection of optimal filters for multispectral imaging, *Applied Optics* **47** (2008), 5585–5591.

[94] Z. Shi and S. Yang, Robust high-order matched filter for hyperspectral target detection, *Electronics Letters* **46** (2010), 1065–1066.

[95] Y. Yagi, Color standardization and optimization in whole slide imaging, *Diagnostic pathology* **6**(Suppl 1) (2011), S15.

[96] D.L. Farkas, C. Du, G.W. Fisher, C. Lau, W. Niu, E.S. Wachman and R.M. Levenson, Non-invasive image acquisition and advanced processing in optical bioimaging, *Comput Med Imaging Graph* **22** (1998), 89–102.

[97] H. Xu and B.W. Rice, *In-vivo* fluorescence imaging with a multivariate curve resolution spectral unmixing technique, *Journal of Biomedical Optics* **14** (2009), 064011.

[98] E. Schrock, S. du Manoir, T. Veldman, B. Schoell, J. Wienberg, M.A. Ferguson-Smith, Y. Ning, D.H. Ledbetter, I. Bar-Am, D. Soenksen, Y. Garini and T. Ried, Multicolor spectral karyotyping of human chromosomes, *Science* **273** (1996), 494–497.

[99] J. Livet, T.A. Weissman, H. Kang, R.W. Draft, J. Lu, R.A. Bennis, J.R. Sanes and J.W. Lichtman, Transgenic strategies for combinatorial expression of fluorescent proteins in the nervous system, *Nature* **450** (2007), 56–62.

[100] M. Sugiyama, A. Sakaue-Sawano, T. Iimura, K. Fukami, T. Kitaguchi, K. Kawakami, H. Okamoto, S. Higashijima and A. Miyawaki, Illuminating cell-cycle progression in the developing zebrafish embryo, *Proceedings of the National Academy of Sciences of the United States of America* **106** (2009), 20812–20817.

[101] A.M. Valm, J.L. Mark Welch, C.W. Rieken, Y. Hasegawa, M.L. Sogin, R. Oldenbourg, F.E. Dewhirst and G.G. Borisy, Systems-level analysis of microbial community organization through combinatorial labeling and spectral imaging, *Proceedings of the National Academy of Sciences of the United States of America* **108** (2011), 4152–4157.

[102] C.M. van der Loos, Multiple immunoenzyme staining: Methods and visualizations for the observation with spectral imaging, *J Histochem Cytochem* **56** (2008), 313–328.

[103] X. Tang, J. He, J. Partin, A. Vafai, Comparative analysis of direct fluorescence, Zenon labeling, and quantum dot nanocrystal technology in immunofluorescence staining, *Journal of immunoassay & immunochemistry* **31** (2010), 250–257.

[104] J.A. Bradford, G. Buller, M. Suter, M. Ignatius, J.M. Beechem, Fluorescence-intensity multiplexing: Simultaneous seven-marker, two-color immunophenotyping using flow cytometry, *Cytometry Part A: The Journal of the International Society for Analytical Cytology* **61** (2004), 142–152.

[105] M.K. Szeszel, C.L. Crisman, L. Crow, S. McMullen, J.M. Major, L. Natarajan, A. Saquib, J.R. Feramisco and L.M. Wasserman, Quantifying estrogen and progesterone receptor expression in breast cancer by digital imaging, *J Histochem Cytochem* **53** (2005), 753–762.

[106] S.J. Rosenthal, J.C. Chang, O. Kovtun, J.R. McBride, I.D. Tomlinson, Biocompatible quantum dots for biological applications, *Chemistry & biology* **18** (2011), 10–24.

[107] E. Tholouli, J.A. Hoyland, D. Di Vizio, F. O'Connell, S.A. Macdermott, D. Twomey, R. Levenson, J.A. Yin, T.R. Golub, M. Loda and R. Byers, Imaging of multiple mRNA targets using quantum dot based *in situ* hybridization and spectral deconvolution in clinical biopsies, *Biochem Biophys Res Commun* **348** (2006), 628–636.

[108] B. Bruhn, J. Valenta, F. Sangghaleh and J. Linnros, Blinking statistics of silicon quantum dots, *Nano letters* **11** (2011), 5574–5580.

[109] X. Shi, Z. Xie, Y. Song, Y. Tan, E.S. Yeung and H. Gai, Superlocalization spectral imaging microscopy of a multicolor quantum dot complex, *Analytical chemistry* **84** (2012), 1504–1509.

[110] P. Hoyer, T. Staudt, J. Engelhardt and S.W. Hell, Quantum dot blueing and blinking enables fluorescence nanoscopy, *Nano letters* **11** (2011), 245–250.

[111] M. Bottrill and M. Green, Some aspects of quantum dot toxicity, *Chemical communications* **47** (2011), 7039–7050.

[112] W. Liu, S. Zhang, L. Wang, C. Qu, C. Zhang, L. Hong, L. Yuan, Z. Huang, Z. Wang, S. Liu, G. Jiang, CdSe quantum dot (QD)-induced morphological and functional impairments to liver in mice, *PloS one* **6** (2011), e24406.

[113] D. Zarkowsky, L. Lamoreaux, P. Chattopadhyay, R.A. Koup, S.P. Perfetto, M. Roederer, Heavy metal contaminants can eliminate quantum dot fluorescence, *Cytometry Part A: The Journal of the International Society for Analytical Cytology* **79** (2011), 84–89.

[114] I.P. Sugar, J. Gonzalez-Lergier and S.C. Sealfon, Improved compensation in flow cytometry by multivariable optimization, *Cytometry A* **79** (2011), 356–360.

[115] *Sequential analysis of biological samples*, US, Editor, 2009.

[116] S. Pierre and K. Scholich, Toponomics: Studying protein-protein interactions and protein networks in intact tissue, *Mol Biosyst* **6** (2010), 641–647.

[117] W. Schubert, A. Gieseler, A. Krusche, P. Serocka and R. Hillert, Next-generation biomarkers based on 100-parameter functional super-resolution microscopy TIS, *N Biotechnol*, 2011.

[118] C. Hennig, N. Adams, G. Hansen, A versatile platform for comprehensive chip-based explorative cytometry, *Cytometry Part A: The Journal of the International Society for Analytical Cytology* **75** (2009), 362–370.

[119] E. Barash, S. Dinn, C. Sevinsky and F. Ginty, Multiplexed analysis of proteins in tissue using multispectral fluores-

cence imaging, *IEEE Trans Med Imaging* **29** (2010), 1457–1462.

[120] S.C. Bendall, E.F. Simonds, P. Qiu, A.D. Amir el, P.O. Krutzik, R. Finck, R.V. Bruggner, R. Melamed, A. Trejo, O.I. Ornatsky, R.S. Balderas, S.K. Plevritis, K. Sachs, D. Pe'er, S.D. Tanner and G.P. Nolan, Single-cell mass cytometry of differential immune and drug responses across a human hematopoietic continuum, *Science* **332** (2011), 687–696.

[121] R.S. Weinstein, The S-curve framework: Predicting the future of anatomic pathology, *Arch Pathol Lab Med* **132** (2008), 739–742.

[122] B.A. Friedman, A survey of the myriad forces changing anatomic pathology and their consequences, *Arch Pathol Lab Med* **132**, 735-738.

[123] V.K. Anagnostou, A.W. Welsh, J.M. Giltnane, S. Siddiqui, C. Liceaga, M. Gustavson, K.N. Syrigos, J.L. Reiter and D.L. Rimm, Analytic variability in immunohistochemistry biomarker studies, *Cancer Epidemiol Biomarkers Prev* **19** (2010), 982–991.

[124] A.J. North, Seeing is believing? A beginners' guide to practical pitfalls in image acquisition, *J Cell Biol* **172** (2006), 9–18.